Applied Radiation and Isotopes 147 (2019) 189–196

Contents lists available at ScienceDirect

Applied Radiation and Isotopes

journal homepage: www.elsevier.com/locate/apradiso

A fuel for generation IV nuclear energy system: Isotopic composition and radiation characteristics

S.V. Bedenko[a,*], N. Ghal-Eh[b,c], I.O. Lutsik[a], I.V. Shamanin[a]

[a] National Research Tomsk Polytechnic University, Tomsk, Russian Federation
[b] School of Physics, Damghan University, Damghan, Iran
[c] Department of Physics, School of Sciences, Ferdowsi University of Mashhad, Mashhad, Iran

HIGHLIGHTS

- Neutronic properties of compound isotope $(Th,Pu)O_2$ as a nuclear fuel were studied.
- Neutron yield and energy spectrum of $(Th,Pu)O_2$ through (α,n) reaction were estimated.
- Analytical calculation method was proposed to characterize the multi-layered spent fuel, $(Th,Pu)O_2$.

ARTICLE INFO

Keywords:
Alpha particle
Isotopic composition
Neutron source
Thorium reactor

ABSTRACT

This paper reports on an important issue of designing appropriate nuclear fuel of a high-temperature gas-cooled nuclear reactor operating in a thorium-plutonium nuclear fuel cycle. The neutronic calculations for a fuel of specific isotopic composition were performed before the analyses were done on the alpha emission probabilities, and on the neutron and photon sources as a result of (α,n) reaction. The main focus was on the quantitative evaluation of the neutron yield and the neutron energy spectrum for the generated neutrons through (α,n) reaction on light nuclei of dispersed nuclear fuel. Tests were carried out with the aim of creating an efficient calculation tool for the initial evaluation of the radiation characteristics for the irradiated multilayer nuclear fuel with different configurations and compositions.

1. Introduction

The physics of a high-temperature gas-cooled low-power thorium reactor facility (HGTRU, Russia) has been studied to explore an optimal configuration of the core and the material composition of the nuclear fuel (Shamanin et al., 2015, 2016, 2018). The investigated reactor (Shamanin et al., 2018) could operate for at least 3000 days at a power of 60 MWth.

The features of reactor core design, the material composition of irradiated nuclear fuel, the operating modes of the reactor and the high burn-up (~400 GWd/tHM) can affect the radiation, nuclear-physical and thermophysical characteristics of spent nuclear fuel (SNF). The revision of the traditional procedures of SNF management seems necessary in order to achieve ultra-high burn-up depth within the nuclear fuel during the stage of reactor design.

Since the concentration of various α-emitters in SNF is directly dependent on the burn-up depth of the nuclear fuel, while the neutron yield of (α,n) reaction depends on the concentration of light elements in the nuclear fuel as well as in the structural materials, it is quite important to understand both the spatial distribution and the probability of (α,n) reaction within the fuel assembly (Vlaskin et al., 2015; Bulanenko, 1979; Murata and Shibata, 2002; Heaton et al., 1989; West and Sherwood, 1982; Simakov and van den Berg, 2017; Shores, 2005). Such studies are basically carried out by means of the commonly-used codes and dedicated programs. However, attention should be made so that the necessary calculations such as the calculations of the isotope composition for the nuclear fuel, the numerical simulation of radiation fields, the development of new procedures and the regulations for SNF management in the nuclear fuel cycle of the new generation (Innovative nuclear systems of the generation VI, 2018) are only possible to undertake with scientific justification and modernization. For example, the ORIGEN-S program (Oak Ridge National Laboratory, USA) (Hermann and Westfall, 1995) can determine the nuclide composition of nuclear fuel as well as the energy spectra of neutrons and photons emitted from SNF, in terms of the given burn-up and holding time.

ORIGEN-S is one of the well-known programs in the world practice

* Corresponding author.
E-mail address: bedenko@tpu.ru (S.V. Bedenko).

https://doi.org/10.1016/j.apradiso.2019.03.005
Received 19 June 2018; Received in revised form 28 February 2019; Accepted 1 March 2019
Available online 06 March 2019
0969-8043/

for the calculation of radiation sources. It is basically used to calculate the burn-up and emission yield of standard oxide fuel (UO_2, $(U,Pu)O_2$) of the light-water reactors (LWR) type. However, in other reactor types and fuels than the standard one, ORIGEN-S may lead to incorrect results.

There are no built-in tools for the calculations of (α,n) reactions in all energy ranges of interest in other widely used codes, such as MCNP5, MCNPX (Los Alamos National Laboratory, USA), KENO-3D (Oak Ridge National Laboratory, USA), MONK (UK), MCU5 (National Research Center, Kurchatov Institute, Russia). Note should be taken that in addition to ORIGEN-S, there are other codes for neutron source calculations such as SOURCES-4C (Los Alamos National Laboratory, USA) (Wilson et al., 2009), NEDIS-2m (VNIINM named after academician A.A. Bochvara, Russia) (Vlaskin and Khomiakov, 2017) and so on (Leniau and Wilson, 2014). These programs, including the commonly-used SOURCES-4C code, are mostly dedicated to the calculations of neutron yield and neutron energy spectrum. Although, SOURCES-4C is a well-recognized program, only a single work was published by its developers in 2009 (Wilson et al., 2009) which was devoted to its capabilities and current status. Comparing to SOURCES-4C, the NEDIS-2m code (Bulanenko, 1979; Vlaskin and Khomiakov, 2017; Spirin et al., 2015) seems to be better adapted to the tasks of modern nuclear power engineering. Therefore, a computational platform for the initial assessment of the radiation characteristics of the nuclear fuel in the nuclear fuel cycle of the new generation seems an urgent task.

Neutrons in nuclear fuels are normally produced through spontaneous and induced fissions, and a result of (α,n) reactions on the light nuclei. In standard oxide fuel (e.g., UO_2) reactors, the (α,n) reaction mainly takes place on $^{17,18}O$ isotopes (Bulanenko, 1979; Spirin et al., 2015). The contribution of (α,n) neutrons does not exceed 20% for LWR-type thermal reactors (Bulanenko, 1979), however, this contribution in the BN-type sodium-cooled fast breeder reactor when using UO_2 as a fuel, reaches 85–95% (Bulanenko, 1979; Spirin et al., 2015).

The nuclear reactor studied in (Shamanin et al., 2018) was a reactor unit for epithermal energy (~63.03% of neutron energies range from 4 eV to 183 keV) and fast-energy (~24.5% of neutron energies range from 183 keV to 20 MeV) neutrons, where $(Th,Pu)O_2$-composition was used as the nuclear fuel. In dispersed nuclear fuels of such a reactor, not only does (α,n) reaction occur on $^{17,18}O$ isotopes, but also do ^{13}C and $^{29,30}Si$ which are contained in micro-fuel coatings (PyC, Ti_3SiC_2) and fuel pellets (SiC). $\chi_{\alpha n}(E)$, the normalized (α,n) neutron spectra, is significantly higher for ^{13}C and $^{29,30}Si$ compared to those in $^{17,18}O$ (Simakov and van den Berg (2017); Shores (2005); Vlaskin and Khomiakov (2017) (Leniau and Wilson, 2014; Spirin et al., 2015; Jacobs and Liskien, 1983); and the carbon (^{13}C) (Hales et al., 2013). The calculations of the energy spectra of spontaneous and induced fission neutrons, $S_{sf}(E)$ and $S_f(E)$, for a mixture of heavy and light isotopes are relatively simple tasks compared to (α,n), $S_{\alpha,n}(E)$. This problem becomes complicated when one deals with spent dispersed nuclear fuel and the media containing different geometry configurations and material compositions (i.e., isotopic neutron sources based on alpha-emitters (Vega-Carrillo and Martinez-Ovalle, 2016; Sogbadji et al., 2014; Elagib et al., 1999), aqueous and alkaline solutions containing different absorbers, etc. (Seale and Andersen, 1991).

For the fresh fuel, $\chi_{\alpha,n}(E)$ and $S_{\alpha,n}(E)$ can be calculated using both available high-precision experimental data (Experimental Nuclear Reaction Data (EXFOR), 2018; Experimental Nuclear Reaction Data (ENSDF), 2018) and the dedicated programs (NEDIS-2.0, SOURCES-4C, SRIM-2013 (Ziegler et al., 2010)). In order to obtain an accurate result, one has to calculate the energy distribution of α-particles, $f_\alpha(E)$, inside the volumes of both the fuel kernel and the coatings (Bedenko et al., 2018; Fomushkin, 2010). The energy distribution $f_\alpha(E)$ can be obtained relying on the following commonly-used assumptions: α-particle sources (i.e., ^{232}Th,$^{239,240,241}Pu$) are uniformly distributed in the core volume which emit the radiation isotropically in the space. The spent fuel kernel is a mixture of unburned isotopes of Pu, Th, minor actinides, oxygen and fission fragments. In such a kernel, the energy distribution functions ($f_\alpha(E)$, $\chi_{\alpha,n}(E)$ and $S_{\alpha,n}(E)$) will depend on the distribution P(E,r) of heavy isotopes and fission products in the volume, for which the use of any other models (Fomushkin, 2010) and extra data requires scientific justification.

In the same vein, the purpose of the present research was the development of an effective calculation tool for the initial assessment of the radiation characteristics of spent fuel within the nuclear fuel cycle of a new generation nuclear energy system. The modeling and numerical calculations were performed with the well-known programs of WIMS-D5B, MCNPX2.6.0, SOURCES-4C and SRIM-2013.

2. Numerical simulations

2.1. Methods and approximations

In general, the neutron energy distributions ($\chi_{\alpha,n}(E)$, $S_n(E)$) depend on several important factors including the geometry of the fuel pellet, the material compositions of the nuclear fuel, the reactor type and its operating modes, as well as the distributions of heavy-metal radiation sources (Pu, Th, minor actinides), $f_{HM}(r)$, fission products, $f_{FP}(r)$ and alpha particles, $f_\alpha(E,r)$, in the fuel kernel, surface and coatings. Three different types of fuel pellets identified as 0817, 1017 and 1200 were used (Shamanin et al., 2018), for which it was proved that an increase in the fuel pellet diameter would lead to the decrease in both the proportion of graphite and the reactivity reserve, $\rho_{inf}(t)$; hence, the core lifetime would depend on both the initial contents of ^{239}Pu, ^{232}Th and the produced isotopes ^{241}Pu and ^{233}U.

The calculations showed that in the fuel pellet type 0817, the ^{239}Pu and ^{232}Th nuclei would burn-out very quickly and the time required for ^{233}U and ^{241}Pu accumulations would be too short to maintain a stationary fission reaction. Therefore, after the 1500 days operation, the ^{239}Pu content would be very small in the reactor which could cause a sudden fall in $\rho_{inf}(t)$. The use of pellet types 1017 and 1200 would result in the accumulation of ^{233}U and ^{241}Pu (in the middle of the irradiation cycle); hence, a longer core lifetime. For fuel pellet types 0817 and 1017, it was noted that the burn-ups of ^{239}Pu were almost identical (about 96–97%). Thus, one may conclude that the best option for a long reactor operation time and the ^{232}Th fuel cycle is the fuel pellet type 1200, despite an increase in the fraction of the disperse phase ($\omega_{fuel} = V_{microfuel} \times N/V_{matrix}$) in this type would cause a decrease in the fraction of burned ^{239}Pu. Moreover, an analysis showed that for a better burn-up of ^{239}Pu, it is necessary to use the fuel pellet of type 1017 (see Fig. 1) (Shamanin et al., 2015, 2016, 2018).

Further neutronic calculations were performed with the program WIMS-D5B as a commonly-used program for cell calculations of different reactor types. The WIMS code uses a set of 69-group neutron energies (14 groups in the fast and 19 in the resonant neutron energy regions) on the basis of the estimated nuclear data files ENDF/B-VII.0 (Aldama Daniel and Trkov, 2000), which allows for the calculations for fast- and thermal-neutron reactors. Since, the geometrical module of WIMS cannot create the hexagonal-shaped cells, the hexagonal cells of HGTRU (Shamanin et al., 2018) were converted into a two-dimensional cylindrical cells. A cylindrical cell is an equivalent Wigner-Seitz cell with given boundary conditions on the surface of the computational zone and the translational symmetry on the both upper and lower faces, with a homogenized fuel cell. In order to calculate the effective multiplication factor (k_{eff}), the axial and radial geometric parameters were introduced by taking into account the transition from the real size of the core to the equivalent Wigner-Seitz system (see Fig. 1b).

The calculations were carried out for 30 different reactor core loading patterns. The heavy metal contents in the fuel pellet cores were as follows: (%): Pu-50, ^{232}Th-50. Pu isotope composition (%): 238-0; 239-94; 240-5.4; 241-0.6; 242-0. The calculation results are illustrated in Fig. 2, which confirms that the increase in ω_{fuel} of more than 17–18% does not lead to a significant increase in reactor operation time, whilst the fraction of burned ^{239}Pu is reduced.

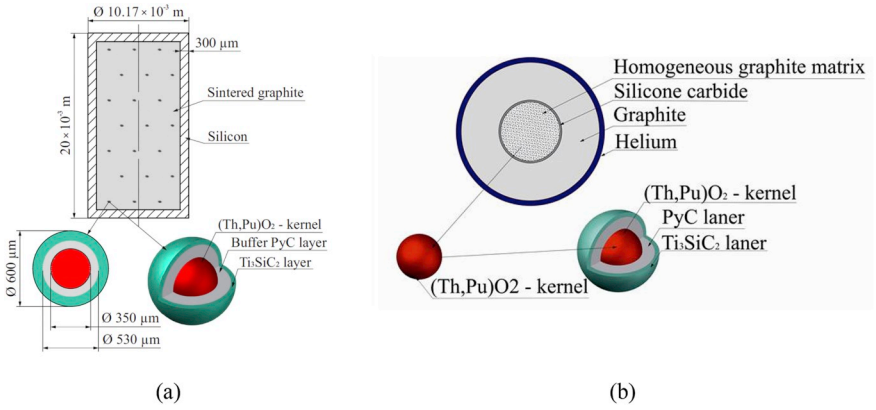

Fig. 1. (a) A 1017 fuel pellet (b) A calculated two-dimensional model of an equivalent cell.

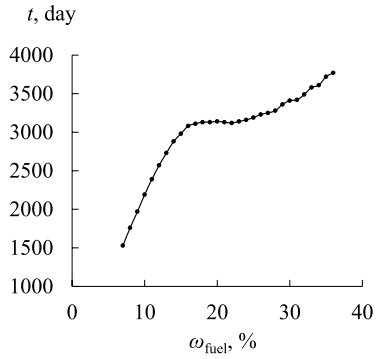

Fig. 2. Duration of operation as a function of fraction of dispersed phase.

It can be noticed from Fig. 2 that the overall nature of the dependency on ω_{fuel} calculated for t, i.e. $t(\omega_{fuel})$, regarding the full-scale heterogeneous reactor model is the same. The results confirm that ω_{fuel} and t do not differ significantly, despite the fact that the homogenization of the fuel cell portion leads to a 3–7% reduction of k_{eff} with respect to a more accurate modeling (Leppänen and DeHart, 2009; Chukbar, 2015).

The calculations showed that for a fuel pellet type of 1017 with ω_{fuel} = 17% and the thermal power of 60 MWth, the reactor operation time would last about 3000 days (see Figs. 2–3).

This configuration burned 84.5%, 36.9% and 9.68% of ^{239}Pu, ^{240}Pu and ^{232}Th, respectively. Since the spent microfuel is a complex mixture

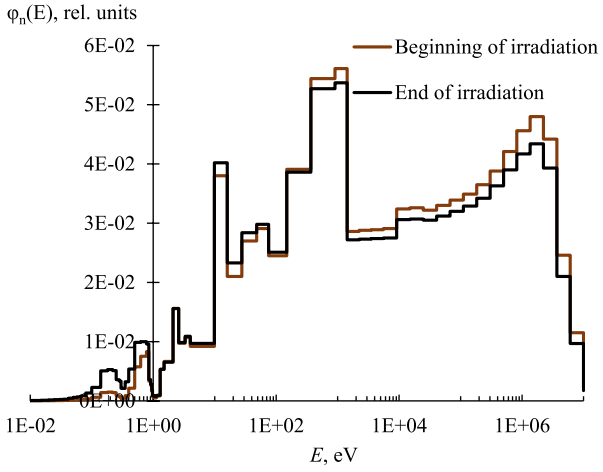

Fig. 3. Variation of neutron flux density versus neutron energy inside the fuel section of the reactor cell at the beginning and the end of irradiation for ω_{fuel} = 17%.

of isotopes, the distribution functions ($f_\alpha(E)$, $\chi_n(E)$ and $S_n(E)$) will depend on the probability density function, P(E,r) which determines how and where the radiation interacts within the kernel volume (Fomushkin, 2010; Bende et al., 1999). The probability density for neutron interaction, $P(l_0,r)$, inside the kernel volume at a distance r from its center can be described by a function of the following form (Fomushkin, 2010; Bende et al., 1999):

$$P(l_0,r) = \int \nu(x,r)\Psi(x)dx \quad (1)$$

here $\nu(x,r)$ is the probability for a neutron interaction in the kernel volume at a distance r from its center; where $\Psi(x)dx = \exp(-x/l_0)dx/l_0$ is the neutron attenuation inside the kernel material following an exponential law; $l_0 = \lambda_t/R$ is the normalized neutron range; λ_t and R are the weighted average of neutron path and kernel radius, respectively. At the beginning and the end of irradiation cycle, the λ_t and l values were $\lambda_{t1} = 1/\Sigma_{t1} = 1/0.309 = 3.24$ cm, $l_{01} = 93$, and $\lambda_{t2} = 1/0.313 = 3.19$ cm, $l_{02} = 91$, respectively. In order to estimate l_0, the weighted average value of neutron mean free path, λ_t, would be calculated based on the assumption that the neutron flux density, $\varphi_n(E)$, remained identical for all fuel pellet materials (i.e., graphite matrix, kernel and coatings) (see Fig. 3). The $P(l_0,r)$ plot for several values of l_0 is shown in Fig. 4.

Fig. 4a shows that the distribution $P(l_0, r)$ for large l_{01} and l_{02} ($\lambda_t \gg R$) is almost uniform ($P(l_{01,02},0)/P(l_{01,02},175) = 1.26$), but it changes significantly from $P(l_{05},r)$ when $\lambda_t \approx R$ (Fig. 4b, line 5). For $\lambda_t \ll R$, the probability $P(l_{03,04}, r)$ is larger in the peripheral part of the kernel (Fig. 4b, line 3 and 4) which accounts for the fission products screening the inner kernel region from the incident neutron flux. This screening effect is well-known for the reactor developers as self-shielding and taken into account by almost all neutron transport programs in the field. Using this model (Fomushkin, 2010), one can estimate the screening effect ($\lambda_t \ll R$), where the corresponding correction

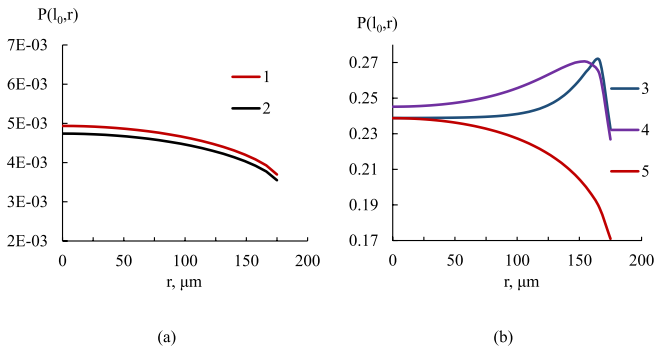

Fig. 4. Probability density function for neutron interactions in the kernel volume: 1 - l_{01} = 91, 2 - l_{02} = 93; l_{03} = 0.1; l_{04} = 0.2; l_{05} = 1.

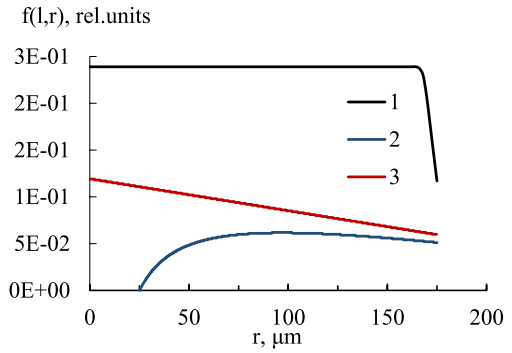

Fig. 5. Spatial distribution of fission fragments in the kernel volume:1 - $l_1 = 0.023$, 2 - $l_2 = 1$; 3 - $l_3 = 1.1$.

will be helpful when the neutron mean free path is much larger than the transverse kernel size ($\lambda_t \gg R$).

Provided that one can assume the heavy isotopes burn out uniformly in the kernel ($P(l_0,r) = 1.26 \approx 1$), at the time the irradiation ends, the α-particles and fission fragments sources are uniformly and homogeneously distributed within the kernel volume. The spatial distribution of fission fragments, $f_{FP}(r)$, can be the determined according to Eq. (2) (Fomushkin, 2010):

$$f_F(l,r) = \begin{cases} \frac{3}{4\pi}, & 0 \le l \le 1-r \\ \frac{3}{4\pi}\left(\frac{1}{2} - \frac{l}{4r} + \frac{1-r^2}{4rl}\right), & 1-r \le l \le 1+r \\ 0, & l \le 1+r \end{cases} \quad (2)$$

where $r = x/R$, $l = \lambda/R$, and λ is the fission products ranges inside the kernel. The average excitation energy of a light ($A_1 = 90$) and heavy ($A_2 = 140$) fragments are about 8 and 10 MeV, respectively. Therefore, the ranges of light products in the kernel material at the end of the irradiation will approximate 4–7 μm ($l_1 = \lambda/R = 4\,\mu m/175\,\mu m = 0.023$) (Ziegler et al., 2010) and their spatial distributions (see Fig. 5, line 1) are independent of r, similar to heavy metals, except for the peripheral layer.

Relying on the calculations above, one can establish the following assumptions: (1) The irradiated core is a homogeneous mixture of heavy isotopes, fission products, and oxygen; (2) The α-particle sources, i.e., the fission products, are uniformly and homogeneously distributed in the kernel; (3) Each source emits the radiation isotropically in the space; and (4) The distribution functions $\chi_{\alpha,n}(E)$ and $S_n(E)$ depend only on the differential energy spectrum of α-particles, $f_\alpha(E) = dN_\alpha(E)/dE$, inside the kernel and on its surface.

2.2. The intensity and energy spectrum of alpha particles

The configuration of the kernel, coatings and fuel pellet is shown in Fig. 1. In order to calculate $f_\alpha(E)$, one has to analyze and solve the problem of radiation emerging from the kernel surface. Similar problems were solved, for example, in (Fomushkin, 2010; Bende et al., 1999; Bak et al., 1965) whose theoretical aspects can be found in the literature on lattice theories. The probability for a radiation to emerge from the core, P, was calculated for a source with self-absorption (Fomushkin, 2010; Bende et al., 1999; Bak et al., 1965):

$$P = \frac{3}{4(\mu R)^3}\left((\mu R)^2 - \frac{1}{2} + \left(\mu R + \frac{1}{2}\right)\exp(-2\mu R)\right) \quad (3)$$

where $\mu = 1/\lambda_0$ is the absorption coefficient, and λ_0 is the mean free path of the radiation. Eq. (3) is valid for any μR wherein the particles (neutrons, γ-ray) mean free path is described by the exponential decay distribution $f(x)dx = \exp(-x/\lambda_0)dx/\lambda_0$. For $\mu R \gg 1$ ($\lambda_0 \ll R$), the first term in (3) contributes, so that $P \approx 3/(4\,\mu R) = 3\lambda_0/(4R)$. The probability P was obtained in (Bak et al., 1965) as a triple integral whose integrand was expanded in a series before an integration-by-part was performed followed by a summation over an infinite series.

In most general cases, such operations are relatively difficult to conduct. However, for $\lambda_0 \ll R$ they become greatly simplified and the solution obtained is also valid for particles with a fixed mean free path (i.e., α-particles, fission fragments, protons). The problem was solved using the principles of geometric probabilities (Fomushkin, 2010). This approach reduces a general problem to the elementary volume calculations which only require the integration of fairly simple functions. Different types of radiation, including radiation with a fixed mean free path was considered in (Fomushkin, 2010). For a radiation of a fixed and relatively small range ($\lambda \le R$), the probability P is given by the formula $P = \frac{3}{4}\frac{\lambda}{R} - \frac{1}{16}\left(\frac{\lambda}{R}\right)^3$, for $\lambda \ll R$, $P \sim 3\lambda/(4R)$.

If the total number of α-particles generated in the kernel at the instant of radioactive decay is $N_{\alpha 0}$, and $P_\alpha(E)$ is the fraction of radiation emitted from the kernel, then the number of α-particles remaining and leaving the kernel are $N_{\alpha 0}(1 - P_\alpha(E))$ and $N_\alpha(E) = N_{\alpha 0} \cdot P_\alpha(E)$, respectively (see Fig. 6a). The differential energy spectrum of α-particles emitted from the kernel surface per unit time into a solid angle 4π is related to $P_\alpha(E)$ relation as follows (see Fig. 6b):

$$f_\alpha(E) = N_{\alpha 0}\frac{dP_\alpha(E)}{dE} = N_{\alpha 0}\cdot\frac{3}{4R}\frac{d\lambda_a(E)}{dE} = N_{\alpha 0}\cdot\frac{3}{4R}\frac{1}{dE}\frac{dE}{(-dE/dx)} = N_{0\alpha}\frac{3}{4}\frac{1}{\varepsilon_\alpha(E)R}. \quad (4)$$

where $\lambda_\alpha(E) = \int dE/(-dE/dx)$ is the range of α-particles in the kernel and $\varepsilon_\alpha(E) = (-dE/dx)$ is the stopping power of α-particles. The mean free path, $1/\lambda_\alpha(E) = \Sigma(w_i/\lambda_{\alpha i})$, and the stopping power

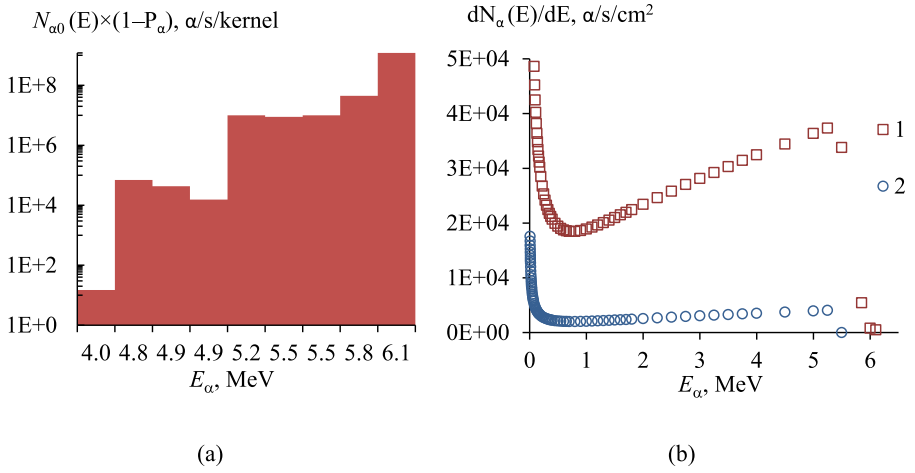

Fig. 6. Energy spectrum of α-particles: (a) At the decay point; (b) From the kernel surface to the solid angle 4π for: 1 - irradiated fuel; 2 - unirradiated fuel.

$\varepsilon_\alpha(E) = \Sigma(w_i \cdot \varepsilon_{\alpha i})$ in the kernel material and in the coating were calculated according to Bragg-Kleeman scaling rule. The mean free path, $R_{\alpha i}(E)$ and the stopping power $\varepsilon_{\alpha i}(E)$ of the i-th nuclide were also calculated using SRIM-2013 program (Ziegler et al., 2010). Fig. 6 shows the energy spectra of α-particles for irradiated and unirradiated fuel. The number of α-particles, $N_{\alpha 0}$, within the kernel of unirradiated fuel pellet (ω_{fuel} = 17%) was ~$2.39 \cdot 10^5$ α/s/kernel, 99.9% of which were generated via the decay of ^{239,240}Pu isotopes, whose average energy was $< E_\alpha > = \Sigma \delta_i \cdot E_i = 5.15$ MeV. The emission probability of α-particles from the kernel surface was $P_\alpha(5.15) = 7.11\%$.

For the irradiated fuel pellet, $N_{\alpha 0} = 3.08 \cdot 10^7$ α/s/kernel, about 99.06% of the α-particles were generated through the decay of the isotopes ^{242,244}Cm, with averaged energy and emission probability of $< E_\alpha > = 5.93$ MeV and $P_\alpha(5.93) = 7.94\%$, respectively. The calculation also showed that the α-particles generated in the kernel of both unirradiated and irradiated fuel pellets remained in the first coating (PyC) since their ranges did not exceed 35 μm (see Fig. 6a). In order to use SOURCES-4C code (Wilson et al., 2009) for further calculations, the continuous spectrum $f_\alpha(E)$ was transformed into energy-group type via the following relation $F^{(i)} = \int_{E_i}^{E_{i+1}} f_\alpha(E)dE$, where i = (0–24), $E_0 = 10^{-4}$ MeV, $E_{24} = 6.2$ MeV.

The SOURCES-4C program conducted the calculation of the intensity and energy spectrum of neutrons produced in both (α,n) and spontaneous fission reactions, as well as the yield and energy spectrum calculations for neutrons generated through the interactions of α-particles of a given energy spectrum within thick targets (Fig. 6b). SOURCES-4C calculated the neutron production using four different models (homogeneous, beam, interface, and three-region problems). In the present work, two model of homogeneous and beam were used.

2.3. Intensity and energy spectrum of the radiation source

The HGTRU hexagonal fuel block was selected for the simulations (Fig. 7) (Shamanin et al., 2015, 2016, 2018). The fuel block was a dense high-quality graphite processed at (3000–3300) K temperature with 76 channels of a small diameter (red color) for fuel pellets of type 1017 (∅10.17×10^{-3} m) and 7 channels (blue color) of a larger diameter (∅24×10^{-3} m) for the heat exchange. The dimensions of the fuel block were 0.207 m width by 0.80 m height.

Fig. 8 shows the calculation results for the neutrons generated inside a single fuel channel with width and height of 10.17×10^{-3} m and 0.8 m, respectively. This fuel channel was filled with pellet type of 1017. The function $S_n(E)$ were prepared in a group form for further calculations with MCNPX2.6.0 (Waters et al., 2007).

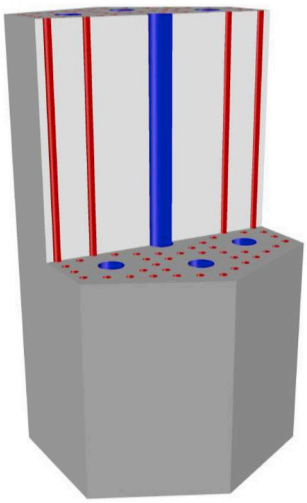

Fig. 7. The 3D model of the HGTRU fuel block.

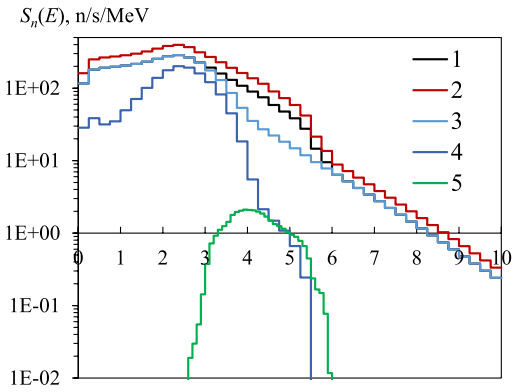

Fig. 8. Energy spectrum of neutrons generated inside the fuel cell: 1, 2 - Total neutron yield for ω_{fuel} = 13 and 17%; 3 - Neutron yield due to spontaneous fission and (α,n) reaction of ^{17,18}O [(Th,Pu)O_2]; 4 - Neutron yield due to (α,n) reaction of ^{17,18}O; 5 - Neutron yield due to the reaction (α,n) of ^{13}C (PyC).

The total neutron yield for ω_{fuel} = 13% (Fig. 8, line 1) and 17% (Fig. 8, line 2) were $3.63 \cdot 10^3$ neutrons/s/basis and ~$4.58 \cdot 10^3$ neutrons/s/basis, respectively. The contributions of neutrons due to the reaction (α,n) on ^{17,18}O oxide fuel ceramics and on ^{13}C (PyC) are 41.1% (Fig. 8, line 4) and 1.18% (Fig. 8, line 5), respectively. $S_{\alpha,n}(E)$ (Fig. 8, line 4) for unirradiated fuels determined the shape of the total distribution of $S_n(E)$ (Fig. 8, lines 1 and 2) which peaked in the energy range of 2.25–2.5 MeV. The peak was due to the (α,n) reaction on the ^{18,17}O nuclei of oxide fuel ceramics; the α-particles were emitted during the decays of ^{239,240,241}Pu and ^{232}Th isotopes.

For irradiated fuel, the total neutron yield $S_n(E)$ could be well approximated by Watt spectral function ($\chi_{sf}(E) = c \cdot \exp(-E/a) \cdot \sinh(bE)^{1/2}$, a = 0.86, b = 3.55, c = 0.35), since the contribution of (α,n)-neutrons did not exceed 0.1%. Moreover, the energy spectrum of photons generated during the decay of ^{239,240,241}Pu and ^{232}Th isotopes was prepared in the ORIGEN-ARP program (Bowman, 2011) according to the energy group format (44GrpORIGEN) (see Fig. 9).

The total photon yields for ω_{fuel} = 13 (Fig. 9, line 1) and 17% (Fig. 9, line 2) were $5.84 \cdot 10^{10}$ photons/s/basis and ~$8.2 \cdot 10^{10}$ photons/s/basis, respectively. More than 99.01% of photons were generated within the energy range of 10–30 keV.

3. Results

As discussed earlier, the energy spectra of the neutron and photon sources (see Figs. 8 and 9) were prepared in an energy group before they were used in the calculations with MCNPX2.6.0 program (Waters et al., 2007). The design of the fuel block and its surface map are shown

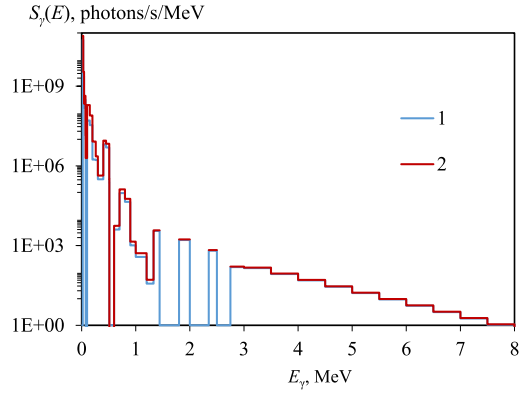

Fig. 9. Energy spectrum of the photons generated inside the fuel cell: 1, 2 – Photon yield for a fuel of ω_{fuel} = 13 and 17%.

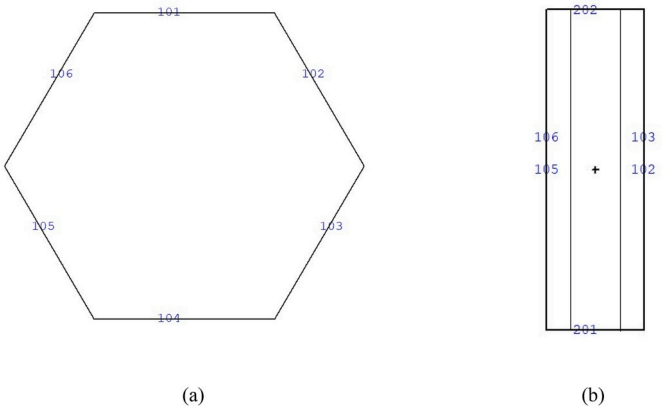

Fig. 10. Surface maps for the computational model of the block; the cross sections in: (a) XY plane; (b) XZ plane.

in Figs. 7 and 10. The fuel block was constructed in the form of a regular hexagonal prism with a width and height of 0.207 m and 0.80 m, respectively (see Fig. 7) (Shamanin et al., 2018). The cylindrical holes designed for the coolant gas filled with air and the temperature of all calculated zones were assumed to be 293.6 K.

The radiation transport calculations were carried out in two stages: Firstly, having considered the source neutron energy spectrum, $S_n(E)$ (Fig. 8), a joint calculation of neutron and photon transport was performed including (n,γ) reaction (see Figs. 11, 12 and 14). At the second stage, the photon transport calculations with the given energy distribution, $S_\gamma(E)$ (Fig. 9), was calculated (Fig. 13). The number of modeled stories was set as 10^9 to keep the relative error for the output values of ($\varphi_n(E)$, k_{eff}) less than 0.03%. Macroscopic cross sections and other nuclear data were taken from the ENDF/B-VII.0. ENDF/B-VI.8 (EPDL97) nuclear data libraries were used to simulate the radiation transport. In addition, nuclear data from the extended ENDF70SAB (model S(α,β)) neutron data library were used for graphite in the thermal energy region.

In order to calculate the neutron flux density, $\varphi_S(E)$, the tally F2 of the MCNPX code was used on the surfaces of the fuel block (Waters et al., 2007). The particles weights outside the fuel block and inside the unit were set to zero (blackbody consideration) and unity, respectively.

The photon flux density, $\varphi_{\gamma i}(E)$, for all lateral surfaces was practically identical (Fig. 13a), whose values for fuel with ω_{fuel} = 13 and 17% were $\varphi_{\gamma 101}(E) = 1.21 \cdot 10^6$ photons/cm^2/s and $2.05 \cdot 10^6$ photons/cm^2/s, respectively. About 99.90% of photon energies were less than 0.6 MeV, with peak value within 0.1–0.2 MeV, with average energies as $< E >$ = 0.137 MeV and 0.134 MeV, for ω_{fuel} = 13% and 17%, respectively. In addition, Fig. 13b shows the total flux density (lines 1 and 2) emerging from all lateral surfaces $\varphi_\gamma(E) = \Sigma\varphi_{\gamma i}(E)$, i = 101–106; line 3

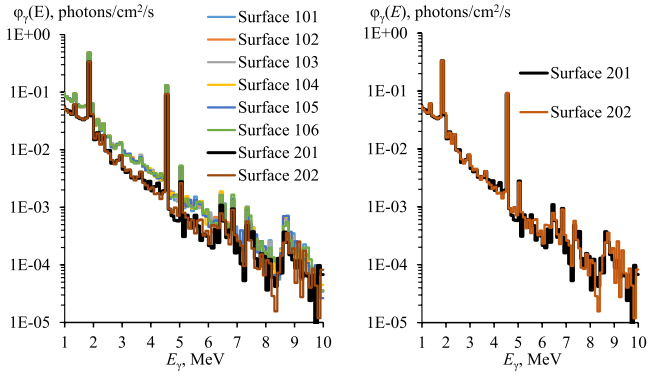

Fig. 11. Photon flux generated through (n,γ) reaction as a function of energy on the surface of the fuel block, ω_{fuel} = 13%.

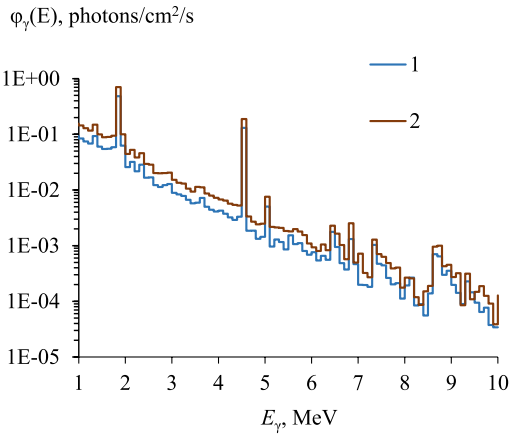

Fig. 12. Photon flux generated through (n,γ) reaction versus photon energy on surface 101: 1 - ω_{fuel} = 13%, 2 - ω_{fuel} = 17%.

- the flux $\varphi_{\gamma 201}(E)$ from the surface 201.

The effective multiplication factor for the fuel block with ω_{fuel} = 13 and 17% was equal to k_{eff} = 0.00981 and ~0.01222, respectively. Thus, the fuel block was a deeply subcritical and nuclear-safe system, and the contribution of neutrons due to multiplication could not exceed 1.2% ($\sim 1/(1-k_{eff}) \approx 1.012$). Therefore, this component of neutron field was not further taken into account.

The total neutron flux densities, $\varphi_n(E)$, emitted from the surface of the fuel block with ω_{fuel} = 13 and 17%, were equal to $\varphi_n(E) = 5.79 \cdot 10^2$ n/cm^2/s (9.86% of the neutrons emitted from the lateral surface 201) and $\sim 8.15 \cdot 10^2$ n/cm^2/s (9.89% of the neutrons emitted from the surface 201), respectively. The neutron energy spectrum, $S_n(E)$, determined the shape of $\varphi_n(E)$ (see Fig. 14), whose peak value fell within the energy regions of 2.51–3.16 MeV, while the average energy for a fuel with ω_{fuel} = 13 and 17% were $< E >$ = 1.65 MeV and ~1.68 MeV, respectively. It was shown that (Plevaka et al., 2015), $\varphi_n(E)$ could be well-approximated by a function as follows: $f(E) = [a(2\pi)^{1/2}]^{-1} \cdot \exp[-(E-b)^2/2a^2]$.

4. Discussion

The MCNPX code is a Monte Carlo program which is frequently used to solve the neutron transport equation whose results when a sufficiently large number of histories are taken into account seem accurate and reliable. When simulating the radiation transport in subcritical systems (Seale and Andersen, 1991; Plevaka et al., 2015; Shamanin et al., 2017) and the media contain discrete multilayer regions (Vega-Carrillo and Martinez-Ovalle, 2016; Sogbadji et al., 2014; Elagib et al.,

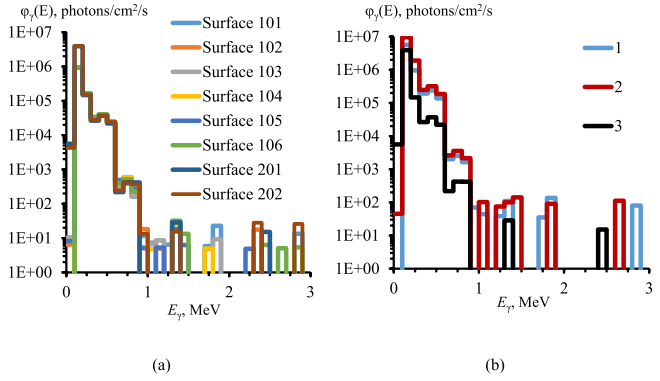

Fig. 13. Photon flux density versus photon energy, for:
(a) fuel with ω_{fuel} = 13%, (b) 1,2 was the total flux density $\varphi_\gamma(E)$ from all lateral surfaces, line 1 was obtained for ω_{fuel} = 13%; line 2 for ω_{fuel} = 17%, 3 was the flux density $\varphi_{\gamma 201}(E)$ for ω_{fuel} = 17%.

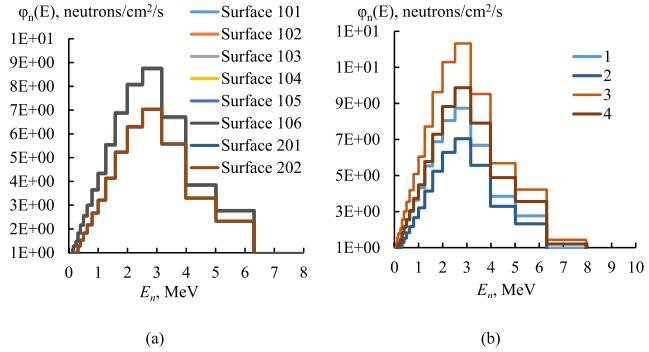

Fig. 14. Variation of neutron flux density versus neutron energy on the surface of the fuel block: (a) ω_{fuel} = 13%; (b) 1, 2 were neutron flux densities at surfaces 101 and 201, respectively, (ω_{fuel} = 13%); 3, 4 were neutron flux density at surfaces 101 and 201 (ω_{fuel} = 17%).

1999), it is necessary to specify not only a large number of neutron histories ($\geq 10^8$), but also to make sure that the output data, including the neutron yield and the (α,n) energy spectrum are accurate enough with relative errors less than 10%.

The fuel block studied in this research was a subcritical multiplying system with a complex internal structure (Fig. 1). In the fuel block of such a reactor, the (α,n) reaction has to be considered not only on the oxygen nuclei (Th,Pu)O_2 composition, but also on the carbon nuclei of the first coating (PyC) of microfuel. To calculate the neutron yield from the coatings, the analytical model proposed in (Fomushkin, 2010; Bende et al., 1999; Bak et al., 1965) and SRIM-2013 program (Ziegler et al., 2010) were used.

This approach is more preferable for preliminary evaluation at the design stage, because it allows the calculations of $f_\alpha(E)$ and $P_\alpha(E)$ in the absence of a simulation code and provide the α-particles to transport from the kernel to the coating (see Fig. 6). Moreover, this approach can be used to generate substantial information, including input data for neutron activation analysis (Vega-Carrillo and Martinez-Ovalle, 2016; Sogbadji et al., 2014; Elagib et al., 1999), the dosimetric parameters of isotope neutron sources (Vega-Carrillo and Martinez-Ovalle, 2016), characteristic data for the design of irradiation facilities (Sogbadji et al., 2014) in multi-source conditions, and other technical problems introduced in (Leniau and Wilson, 2014; Spirin et al., 2015; Elagib et al., 1999; Seale and Andersen, 1991; Bende et al., 1999). The accuracy of the calculations can be improved by incorporating updated cross-section data of (α,xn) reactions, the more reliable data on the stopping powers and other recommendations provided in (Vlaskin et al., 2015; Murata and Shibata, 2002; Simakov and van den Berg, 2017; Shores, 2005; Wilson et al., 2009; Leniau and Wilson, 2014).

5. Conclusions

In the present work, the fundamental issue of handling nuclear fuel in a high-temperature gas-cooled thorium reactor plant operating in the thorium-plutonium nuclear fuel cycle was studied. Both the neutronic and isotope composition calculations of the fuel were performed in the study, and the α-emitters, neutron and photon sources were analyzed. Furthermore, the energy spectra of the radiation sources (Figs. 6, 8 and 9) were prepared in an energy group format for more calculations with the MCNPX2.6.0 code. The results are illustrated in Figs. 11–14. The main focus was on the quantitative evaluation of neutron yield and neutron energy spectrum (Fig. 8), following the (α,n) reaction on light nuclei of spent nuclear fuel (Fig. 1).

The research was conducted with the purpose of creating an efficient calculation tool used for the initial assessment of the radiation characteristics for a nuclear fuel in the new-generation nuclear fuel cycle. This enabled the investigation of the radiochemical and corrosion resistance of the elements used in the transport container design. Despite the approach used in this study was economical in terms of computational costs, it can effectively be used to solve various applied problems of modern nuclear power engineering.

Acknowledgements

The work was supported by Russian Science Foundation № 18-19-00136 of April 18, 2018, for the project titled “Scientific basis development of oxide compositions plasma-chemical synthesis technology for perspective nuclear fuel types”.

Appendix A. Supplementary data

Supplementary data to this article can be found online at https://doi.org/10.1016/j.apradiso.2019.03.005.

References

Aldama Daniel, L., Trkov, A., 2000. Analysis of the burnup credit benchmark with an updated WIMS-D library. Ann. Nucl. Energy 27 (2), 169–174. https://doi.org/10.1016/S0306-4549(99)00061-4.
Bak, M.A., Petrzhak, K.A., Romanov, Yu F., 1965. Spherical source irradiation under self-shielding. Tech. Phys. Russ. J. Appl. Phys. 26 (2), 379–384 (in Russia).
Bedenko, S., Shamanin, I., Grachev, V., Knyshev, V., Ukrainets, O., Zorkin, A., 2018. Neutron radiation characteristics of the IVth generation reactor spent fuel. AIP Conf. Proc. 1938 (020001). https://doi.org/10.1063/1.5027208.
Bende, E.E., Hogenbirk, A.H., Kloosterman, J.L., Van Dam, H., 1999. Analytical calculation of the average dancoff factor for a fuel kernel in a pebble bed high-temperature reactor. Nucl. Sci. Eng. 133 (2), 147–162. https://doi.org/10.13182/NSE99-A2078.
Bowman, S.M., 2011. Scale 6: comprehensive nuclear safety analysis code system. Nucl. Technol. 174 (2), 126–148. https://doi.org/10.13182/NT10-163.
Bulanenko, V.I., 1979. Neutron yield of (α,n) reaction on oxygen. Sov. Atom. Energy 47 (1), 531–534. https://doi.org/10.1007/BF01133430.
Chukbar, B.K., 2015. Verification of statistical method CORN for modeling of microfuel in the case of high grain concentration. Phys. Atom. Nucl. 78 (11), 1200–1205. https://doi.org/10.1134/S1063778815110071.
Elagib, I., Csikai, J., Jordanova, J., Oláh, L., 1999. Leakage neutron spectra from spherical samples with a Pu-Be source. Appl. Radiat. Isot. 51 (3), 329–333. https://doi.org/10.1016/S0969-8043(99)00046-9.
Evaluated Nuclear Structure Data File. http://www.nndc.bnl.gov/ensdf, Accessed date: 4 April 2018.
Experimental Nuclear Reaction Data. https://www-nds.iaea.org/exfor/exfor.htm, Accessed date: 8 April 2018.
Fomushkin, E.F., 2010. Some characteristics of radiation distribution in the spherical active system. Quest. Atom. Sci. Technol. : Phys. Nucl. React. 2, 17–21 (in Russian).
Hales, J.D., Williamson, R.L., Novascone, S.R., Perez, D.M., Spencer, B.W., Pastore, G., 2013. Multidimensional multiphysics simulation of TRISO particle fuel. J. Nucl. Mater. 443 (1–3), 531–543. https://doi.org/10.1016/j.jnucmat.2013.07.070.
Heaton, R., Lee, H., Skensved, P., Robertson, B.C., 1989. Neutron production from thick-target (α,n) reactions. Nucl. Instrum. Methods Phys. Res. 276 (3), 529–538. https://doi.org/10.1016/0168-9002(89)90579-2.
Hermann, O.W., Westfall, R.M., 1995. ORIGEN-S: SCALE System Module to Calculate Fuel Depletion, Actinide Transmutation, Fission Product Buildup and Decay, and Associated Radiation Source Terms. Vol. II, Sect. F7 of SCALE: A Modular Code System for Performing Standardized Computer Analyses for Licensing Evaluation. NUREG/CR-0200 Rev.
Innovative nuclear systems of the generation VI. http://www.atomic-energy.ru/technology/34307, Accessed date: 17 April 2018.
Jacobs, G.J.H., Liskien, H., 1983. Energy spectra of neutrons produced by α-particles in thick targets of light elements. Ann. Nucl. Energy 10 (10), 541–552. https://doi.org/10.1016/0306-4549(83)90003-8.
Leniau, B., Wilson, J.N., 2014. A new spent fuel source characterization code CHARS and its application to the shielding of the thorium. Prog. Nucl. Sci. Technol. 4, 134–137. https://doi.org/10.15669/pnst.4.134.
Leppänen, J., DeHart, M., 2009. HTGR reactor physics and burnup calculations using the serpent Monte Carlo code. Trans. Am. Nucl. Soc. 101, 782–784.
Murata, T., Shibata, K., 2002. Evaluation of the (α,n) reaction nuclear data for light nuclei. J. Nucl. Sci. Technol. 39, 76–79. https://doi.org/10.1080/00223131.2002.10875044.
Plevaka, M.N., Bedenko, S.V., Gubaidulin, I.M., Knyshev, V.V., 2015. Neutron-physical studies of dry storage systems of promising fuel compositions. Bull. Lebedev Phys. Inst. 42 (8), 240–243. https://doi.org/10.3103/S1068335615080059.
Seale, R.L., Andersen, R.E., 1991. Intrinsic neutron source strengths in uranium solutions. Trans. Am. Nucl. Soc. 63, 226 1991.
Shamanin, I., Bedenko, S., Chertkov, Y., Gubaydulin, I., 2015. Gas-cooled thorium reactor with fuel block of the unified design. Adv. Mater. Sci. Eng. 2015 (392721). https://doi.org/10.1155/2015/392721.
Shamanin, I.V., Bedenko, S.V., Chertkov, YuB., 2016. Thorium-loaded low-power reactor installation operated with super-long fuel residence time. Izvestiya Wysshikh Uchebnykh Zawedeniy, Yadernaya Energetika 2, 121–132.

Shamanin, I.V., Bedenko, S.V., Nesterov, V.N., Lutsik, I.O., Prets, A.A., 2017. Solution of neutron-transport Multigroup equations system in subcritical systems. Izvestiya Wysshikh Uchebnykh Zawedeniy, Yadernaya Energetika (4), 38–49. https://doi.org/10.26583/npe.2017.4.04.

Shamanin, I.V., Grachev, V.M., Chertkov, Y.B., Bedenko, S.V., Mendoza, O., Knyshev, V.V., 2018. Neutronic properties of high-temperature gas-cooled reactors with thorium fuel. Ann. Nucl. Energy 113, 286–293. https://doi.org/10.1016/j.anucene.2017.11.045.

Shores, E.F., 2005. Plutonium oxide benchmark problems for the SOURCES code. Appl. Radiat. Isot. 62 (5), 699–704. https://doi.org/10.1016/j.apradiso.2004.12.002.

Simakov, S.P., van den Berg, Q.Y., 2017. Update of the α-n yields for reactor fuel materials for the interest of nuclear safeguards. Nucl. Data Sheets 139, 190–203. https://doi.org/10.1016/j.nds.2017.01.005.

Sogbadji, R.B.M., Abrefah, R.G., Nyarko, B.J.B., Akaho, E.H.K., Odoi, H.C., Attakorah-Birinkorang, S., 2014. The design of a multisource americium-beryllium (Am-Be) neutron irradiation facility using MCNP for the neutronic performance calculation. Appl. Radiat. Isot. 90, 192–196. https://doi.org/10.1016/j.apradiso.2014.03.017.

Spirin, E.V., Aleksakhin, R.M., Vlaskin, G.N., Utkin, S.S., 2015. Radiation balance of spent nuclear fuel of a fast reactor and natural uranium. Atom. Energy 119 (2), 142–148. https://doi.org/10.1007/s10512-015-0040-4.

Vega-Carrillo, H.R., Martinez-Ovalle, S.A., 2016. Few groups neutron spectra, and dosimetric features, of isotopic neutron sources. Appl. Radiat. Isot. 117, 42–50. https://doi.org/10.1016/j.apradiso.2016.03.027.

Vlaskin, G.N., Khomyakov, Y.S., Bulanenko, V.I., 2015. Neutron yield of the reaction (α,n) on thick targets comprised of light elements. Atom. Energy 117 (5), 357–365. https://doi.org/10.1007/s10512-015-9933-5.

Vlaskin, G., Khomiakov, Y., 2017. Calculation of neutron production rates and spectra from compounds of actinides and light elements. EPJ Web Conf. 153 (07033). https://doi.org/10.1051/epjconf/201715307033.

Waters, L.S., McKinney, G.W., Durkee, J.W., 2007. The MCNPX Monte Carlo radiation transport code. AIP conf. Proc. 896, 81–90. https://doi.org/10.1063/1.2720459.

West, D., Sherwood, A.C., 1982. Measurements of thick-target (α,n) yields from light elements. Ann. Nucl. Energy 9, 551–577. https://doi.org/10.1016/0306-4549(82)90001-9.

Wilson, W.B., Perry, R.T., Charlton, W.S., Parish, T.A., 2009. Sources: a code for calculating (alpha,n), spontaneous fission, and delayed neutron sources and spectra. Prog. Nucl. Energy 51 (4–5), 608–613. https://doi.org/10.1016/j.pnucene.2008.11.007.

Ziegler, J.F., Ziegler, M.D., Biersack, J.P., 2010. SRIM - the stopping and ranges of ions in matter. Nucl. Instrum. Methods Phys. Res. B 268, 1818–1823. https://doi.org/10.1016/j.nimb.2010.02.091.